



SBE21

Sustainable Built Heritage

14-16 April 2021,
Online conference

DRAFT PAPER

This version is intended for personal use during the conference and may not be divulged to others

The SBE21 Heritage Conference is co-financed by:



International co-promoters:



Under the patronage of:



In collaboration with:



Hygrothermal analysis of a wall isolated from the inside: the potential of dynamic hygrothermal simulation

S Panico^{1,2}, M Larcher^{1,3}, A Troi¹, I Codreanu^{1,2}, C Baglivo² and P M Congedo²

¹ Institute for Renewable Energies, Eurac Research, Viale Druso 1, 39100 Bolzano, Italy

² Department of Engineering for Innovation, University of Salento, 73100 Lecce, Italy

³ Corresponding author, marco.larcher@eurac.edu

Abstract. Hygrothermal simulations are expected to provide powerful support to the design process in the context of energy retrofit of historic buildings and prevent the moisture-related damages. They can be used to predict the hygrothermal behaviour of the building in detail and exclude the occurrence of moisture related damages, such as mould formation or material degradation. However, these simulations require various input data related to materials and boundary conditions, which are often difficult to find during the design phase. In this article we analyse the potential of hygrothermal simulations in predicting the hygrothermal behaviour of an internally insulated wall, even with limited information on the hygrothermal properties of the materials composing the historical wall. The quality of the simulation's results is evaluated through a comparison with monitored data. The numerical model is calibrated to maximise the agreement with the monitored data. The considered case study is a historical building located nearby Bolzano (Northern Italy). The monitoring system is installed with the aim of analysing temperature and relative humidity profiles within the construction. In addition, the climatic boundary conditions are measured both inside and outside the building, including temperature, relative humidity, driving rain and solar radiation. The numerical simulation of the wall under analysis is performed with the software DELPHIN.

Keywords – Hygrothermal Numerical Simulation, Monitoring, Calibration, Sensitivity Analysis

1. Introduction

A building is a very complex system whose walls are influenced by several factors: temperature variation, relative humidity, solar radiation, wind, and rain generate a flow of heat and moisture inside the materials that compose the wall. The phenomena that come into action are mainly accumulation and transport processes. Both are due to heat and humidity. In particular, the transport of moisture in building materials can take place either in the form of vapour diffusion or in the form of capillary liquid transport. The latter is generally due to possible sources of rain, condensation, or rising damp.

The presence of excessive moisture levels in buildings can potentially have an impact on the indoor environmental quality as well as the aesthetics and structural integrity of materials and hence affect both the conservation and the performance of buildings. Some of the most commonly found moisture related damages in construction are: frost damage, damage due to crystallization of salts, biological attack (from the growth of mould to dry and wet rot), or corrosion of steel in reinforced concrete structures [1]. Water management in buildings is therefore one of the most important factors related to the longevity of buildings. The moisture content of building materials can also significantly influence their thermal performance. Building materials with a high moisture content can cause a 2-9% increase in heat loss due to increased thermal conductivity and latent heat effects [2]. The addition of insulation on the internal side of walls in cold and humid climates can accelerate the performance and durability problems

above [3]. It is therefore important to carry out forecasts that can safeguard the building to be renovated. The tool used for this purpose is the hygrothermal analysis. This work follows the hygrothermal simulation in dynamic regime (EN 15026) method and uses an advanced tool for the simulation of the combined transport of moisture and heat in building components. The advanced dynamic model offers the possibility to perform hourly dynamic hygrothermal simulations and considers the capillary transport of liquids and the moisture storage properties of materials. The use of this method makes it possible to study in detail all the above-mentioned moisture damages. At the same time it requires expertise, information on building materials and indoor and outdoor climatic data. To obtain these data, a monitoring system was developed to provide the necessary information for a dynamic simulation. It was possible to record a series of data coming from sensors placed in a retrofitted historical building. Using real data from the sensors, an attempt was made to calibrate the numerical model with the objective of figuring out which parameters have the greatest influence on the model.

This work is to be considered as a preliminary approach in which based on monitored data, parametric simulations are launched by varying only one parameter at a time for each material. Moreover, only few works have investigated the thermo-hygrometric calibration of materials. A similar work was done from Freudenberg et al. [4] which the thermal conductivity of the insulation (λ_{ins}), the hygric and the thermal transfer coefficients were calibrated using the GENOPT optimization software on a sample wall under controlled conditions for 6 days. Roberti et al. [5] conducted an interesting work combining a sensitivity analysis with an optimization on a case study monitored for about 6 months. Grint et al. [6] have varied several parameters to define how they affect the RH. Comparing the monitored data with simulated data for over a year, Coelho et al. [7] highlighted the importance of using outdoor climate data as close as possible to the case study; in this work the calibrated parameters are: the air change rate, the short-wave radiation absorption coefficient of exterior walls and the solar heat gain coefficient of the windows.

2. Methods

This work presents the calibration of a numerical model describing the hygrothermal behavior of an internally insulated historical wall. The numerical model is set up within the software DELPHIN 6.1 [8] while the monitored data are obtained from a fully operative building that is acting as a living lab.

2.1. The Case Study and the Monitoring System

The analyzed case study is located in Settequerce/Siebeneich (BZ) in South Tyrol (Alto Adige/Südtirol) area and is currently being used as a single-family house. In 2017, the building was retrofitted and the walls were insulated from the inside with a vapor-open insulation system. The red porphyry stone walls have a thickness of 44 cm while the insulation system is a wood fiber panel with a thickness of 8 cm. The insulation panels were attached to the existing interior plaster using an adhesive clay mortar (1 cm) that is applied directly on the existing interior plaster. A new lime plaster was applied as a finishing layer, both inside (approximately 1.5 cm) and outside (approximately 2 cm). The wall build-up before and after renovation is shown in Figure 1.

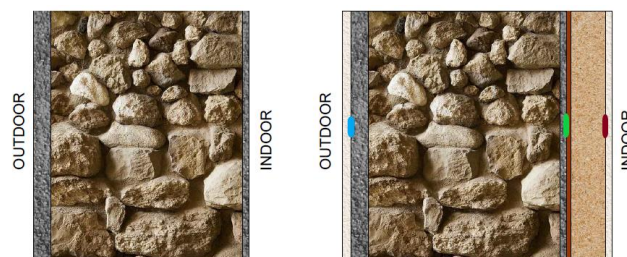


Figure 1. Stratigraphy of the monitored wall before (left) and after (right) the renovation work. The location of the installed sensors within the stratigraphy is indicated by the colored vertical bars.

During the renovation, sensors were placed in the wall stratigraphy, in the exterior environment and inside the adjacent room. The Northeast facing wall (62° North) was chosen for this monitoring. The analysed monitoring period is 1 year and 9 months. Combined temperature and relative humidity sensors were placed within the stratigraphy to monitor the hygrothermal conditions inside the wall. Their exact location is shown in the right part of Figure 1. A set of two sensors is located between the old plaster and the new plaster (blue), two sensors are inserted in the glue layer under the insulation (green), and a third set of two sensors is inserted between the insulation and the new plaster (red). These positions were chosen to best describe the stratigraphy from a hygrothermal point of view. The sensors combine an NTC thermistor and a capacitive humidity sensor with an accuracy of $\pm 0.3\text{ }^{\circ}\text{C}$ and $\pm 2.5\%$, respectively.

In the room adjacent to the wall, a combined temperature and relative humidity sensor was placed to monitor the conditions inside the building. In the exterior environment, a temperature and relative humidity sensor, a pyranometer for solar radiation reading, and a tipping bucket rain gauge for the acquisition of driving rain data were installed. All sensors are connected to an acquisition system with dedicated software that allows collecting all monitoring data.

2.2. Simulation and Calibration

The software DELPHIN 6.1 describes the combined transport of heat and moisture in building components in dynamic regime, giving the possibility of simulating their hygrothermal behavior according to the standard EN 15026 [9]. For the creation of these numerical models three types of input are typically required: hygrothermal properties of building materials, boundary conditions (i.e. interior and exterior climate) and some coefficients describing the coupling of the construction with the boundary conditions.

In our case the boundary conditions are monitored on-site, as described in the previous subsection providing an almost exact data set. This represents a huge advantage with respect to the typical situation where the external climatic conditions are derived from climatic stations close to the building and the internal conditions are estimated with simplified theoretical models [10], [9]. The other two input types, i.e. the material properties and the coupling coefficients, are instead calibrated through a parametric analysis. Moreover, laboratory tests, as well as the data extracted from the material datasheet, are used as support for this analysis. The calibration procedure is implemented in 3 phases:

Phase 1: in this phase, it is set up a preliminary numerical model that will then be refined in the following phases. For the first simulation, materials are chosen from the DELPHIN database according to a qualitative analysis, trying to match the description in the database with the information gathered on-site and on the datasheets. Moreover, priority is given to those materials with hygrothermal properties close to those present in the datasheets of the materials used for the intervention. For the insulation, the same material used in the case study is found in the database. The new applied plaster is based on hydraulic lime, the plaster selected from DELPHIN's database is also a hydraulic lime plaster used for levelling irregular wall surfaces. The glue is chosen so that its hygrothermal properties are as close as possible to those in the datasheet. The stone that forms the load-bearing part of the masonry is a red sandstone whose specific heat, density and thermal conductivity values were measured in the laboratory. Based on these values, Sandstone Karlshafener was identified. As there is no information about the existing old plaster, the choice of material was particularly difficult. In fact, since there is no value of the physical parameters, a lime plaster present in the database was chosen. The values of the heat transfer coefficients, h_{in} and h_{out} , and of the vapor exchange coefficients, β_{in} and β_{out} are taken from the literature [10]. In particular, the following values are chosen $h_{in} = 8 \frac{\text{W}}{\text{m}^2\text{K}}$, $h_{out} = 17 \frac{\text{W}}{\text{m}^2\text{K}}$, $\beta_{in} = 2.5 \times 10^{-8} \text{ s/m}$ and $\beta_{out} = 7.5 \times 10^{-8} \text{ s/m}$. The overall driving rain reduction coefficient, R_r , is estimated based on the standard EN ISO 15927-3 [11] to have a value of 0.18. The solar radiation absorption coefficient, a_{sw} , is set to 0.4, which corresponds to a light-colored paint.

Phase 2: in this phase a first parametric analysis is performed. In particular, for every layer of the wall build up several materials taken from the DELPHIN database are tried in the simulation and the one giving the “best” result is selected. The “best” result is defined as the one minimizing an objective function based on the sum of the root-mean-square-errors (RMSE) of all the hygrothermal parameters

measured within the stratigraphy. More precisely, for every one of the 3 monitored positions the RMSE is calculated both for the temperature, T , and for the relative humidity, φ :

$$RMSE_T = \sqrt{\frac{1}{N} \sum_i \left(\frac{T_{i,mon} - T_{i,sim}}{e_{T_{i,mon}}} \right)^2} \quad RMSE_\varphi = \sqrt{\frac{1}{N} \sum_i \left(\frac{\varphi_{i,mon} - \varphi_{i,sim}}{e_{\varphi_{i,mon}}} \right)^2}$$

where the index, i , represents a sum of all the simulated/monitored hours. The monitored parameter ($T_{i,mon}$ or $\varphi_{i,mon}$) for each position is calculated as the average of the two sensors performing the measurement in that layer. The difference between the monitored parameter and the simulated parameter is divided by the measurement error, $e_{i,mon}$, which in general depends on the hour, i , since it is calculated as the maximum between the sensor accuracy and the statistical error of the 2 sensors measuring that parameter in that specific layer. The final objective function is calculated as the sum of $RMSE_T$ and $RMSE_\varphi$ for all the 3 monitored positions. This procedure is carried out for all the materials composing the stratigraphy. The procedure is first applied to the stone, then the new plaster, the existing plaster and finally the glue. The insulation layer is not included in this procedure since there is an exact correspondence between the material installed on-site and the one present in the database. Each material is varied keeping the others constant and the one returning the lowest objective function is selected.

Phase 3: as a final step of the calibration procedure the single hygrothermal parameters of the materials are adjusted as well as the coupling coefficient with the interior and the exterior environment.

As regards the material parameter, in this paper, we focus our attention on the three parameters that we expect to influence the most the simulation results: the specific heat capacity, c_p , the thermal conductivity, λ_{dry} , and the vapor diffusion resistance factor, μ_{dry} . Whenever a parameter is known from the material datasheet, it is adjusted accordingly in the numerical model. Conversely, if the parameter is not known, a parametric analysis is performed and the value minimizing the objective function is selected. The parameter adjustments are performed one at a time in the order reported in Table 4. In the same table the variation range as well as the variation step are also reported. As regards the variation of μ_{dry} and λ_{dry} an additional specification is required. In DELPHIN, vapor diffusion and thermal transport in materials are not described by a single parameter (λ_{dry} or μ_{dry}) but by two functions which depends on the moisture content, θ_l : the vapour conductivity function, $k_v(\theta_l)$, and the thermal conductivity function $\lambda(\theta_l)$ which are related to λ_{dry} and μ_{dry} by the following equations [8].

$$k_v(\theta_l) = \frac{D_{v,air}}{R_v T \mu(\theta_l)} \quad \text{where } \mu_{dry} = \mu(\theta_l = 0) \text{ and } D_{v,air}, \text{ is the vapour diffusivity} \\ \text{of air and is given by the Schirmer equation} \quad (1)$$

$$\lambda(\theta_l) = \lambda_{dry} + 0.56 \theta_l. \quad \text{where } \lambda_{dry} = \lambda(\theta_l = 0) \quad (2)$$

When the μ_{dry} value is changed from its *old* value to a *new* value the $k_v(\theta_l)$ function is recalculated according to the following logarithmic scaling:

$$\log[k_v^{new}(\theta_l)] = \log[k_v^{old}(\theta_l)] \frac{\log[k_v^{new}(0)]}{\log[k_v^{old}(0)]} \quad k_v^{new/old}(0) = \frac{D_{v,air,R}}{R_v T_r \mu_{dry}^{new/old}} \quad (3)$$

After the adjustment of the material's parameter the coupling coefficient with the indoor and outdoor environment ($h_{in}, h_{out}, \beta_{in}, \beta_{out}$ and a_{sw}) are adjusted with a parametric analysis. Also, in this case, the parameter variation is performed one at a time and keeping the other values fixed. The variation order, the variation range as well as the variation step are reported in Table 4.

3. Results

In Table 1., Table 2. and Table 3. we report the materials that are selected in the numerical simulation after *Phase 1*, *Phase 2* and *Phase 3* respectively. In the same tables we also report the corresponding hygrothermal properties of the materials: specific heat capacity c_p , thermal conductivity λ_{dry} , and vapour diffusion resistance factor μ_{dry} .

Table 1. Starting materials assigned for the simulation

Base materials				
Materials	Code	cp [J/kg·K]	λ [W/m·K]	μ [-]
New Plaster	(722)	802	0.680	9.26
Insulation	(270)	2000	0,042	3
Glue	(677)	889	0,724	10,26
Old Plaster	(520)	869	0.690	18.96
Stone	(563)	796	3277	178.5

Table 2. Materials that performed better (yellow) after parametric analysis

Best materials				
Materials	Code	cp [J/kg·K]	λ [W/m·K]	μ [-]
New Plaster	(628)	999	0.281	12.14
Insulation	(270)	2000	0,042	3
Glue	(677)	889	0,724	10,26
Old Plaster	(252)	1418	0.619	50.98
Stone	(469)	708	2000	12.98

Table 3. In grey the parameters adapted to the documentation and in green the values of the parameters obtained after the parametric simulations

Parametric Analysis				
Materials	Code	cp [J/kg·K]	λ [W/m·K]	μ [-]
New Plaster	(628)	830	0,63	12,5
Insulation	(270)	2100	0,043	3
Glue	(677)	889	1,1	10,26
Old Plaster	(252)	1600	1,1	38
Stone	(469)	850	1,5	5

Table 1 shows the starting materials chosen for simulation with their related parameters. After varying the materials in parametric form, materials that reduced the RMSE index are obtained. The replaced materials are highlighted in yellow (Table 2). The glue is the only unchanged parameter in *Phase 2* since the material selected in *Phase 1* is already the optimal one. The last table (Table 3) highlights the parameters modified to fit the available datasheet values (values in grey) and those obtained after the parametric analysis (in green). That allowed to improve the simulated curves by approaching them to the monitored ones.

Table 4. Steps performed during the parametric analysis process.

Phases	Materials	Parameters	Range variation	Initial Value	Best	Thermal RMSE	Hygrometric RMSE	
<i>Phase 1</i>	Base materials	[-]	\	[-]	[-]	9,27	6,56	
<i>Phase 2</i>	Stone	materials	\	Sandstone Karlshafener [563]	Sandstone Rütthen [469]	8,8	4,75	
	New plaster		\	Inside lime plaster [722]	Lime Plaster fine [628]	7,91	5,1	
	Existing plaster		\	Lime plaster	Surface plaster	7,67	4,89	
	Glue		\	Loam Adhesive	Loam Adhesive	7,67	4,89	
<i>Phase 3</i>	Datasheets adaptation values			Table 2	Table 3 (gray parameters)	8,57	4,92	
	Stone	λ [W/m·K]	0,3 ÷ 3,5 (0,1)	2	1,5	8,17	5,01	
	Existing plaster		0,1 ÷ 1,1 (0,1)	0,619	1,1	7,81	4,95	
	Stone		200 ÷ 1000 (50)	700	850	7,72	4,95	
	Existing plaster	cp [J/kg·K]	400 ÷ 1600 (50)	1418	1600	7,65	4,95	
	Glue		700 ÷ 1400 (50)	889	889	7,65	4,95	
	Stone	μ [-]	5 ÷ 180 (5)	12,98	5	7,63	4,81	
	Existing plaster		5 ÷ 55 (5)	50,98	38	7,62	4,81	
		h _{in}	h [W/m²K]	1 ÷ 15 (0,5)	8	3,5	6,96	4,27
				h _{out}	10 ÷ 25 (0,5)	17	25	6,66
		β _{in}	β [s/m] · 10 ⁻⁸	1 ÷ 5,5 (0,2)	12,5	5,4	6,66	3,77
				β _{out}	1 ÷ 17 (0,5)	7,5	25	6,66
		α _{sw}	[-]	0 ÷ 1 (0,05)	0,4	0,2	6,32	3,55

Table 4 represents in detail how the RSME index has changed for each step performed in the calibration process. The "thermal RMSE" value represents the sum of the indices obtained for the three sensors in terms of temperature while "Hygrometric RMSE" in terms of relative humidity. The following graphs show the behaviour of the simulated and monitored relative humidity curves in the three analysed positions. The red curves represent the monitored one and the shaded areas represent the error of the sensors calculated as the greater of the sensor error (from the datasheets) and the statistical error. The green, blue and black curves represent instead the simulated curves respectively after *Phase 1*, *Phase 2* and *Phase 3* of the calibration process.

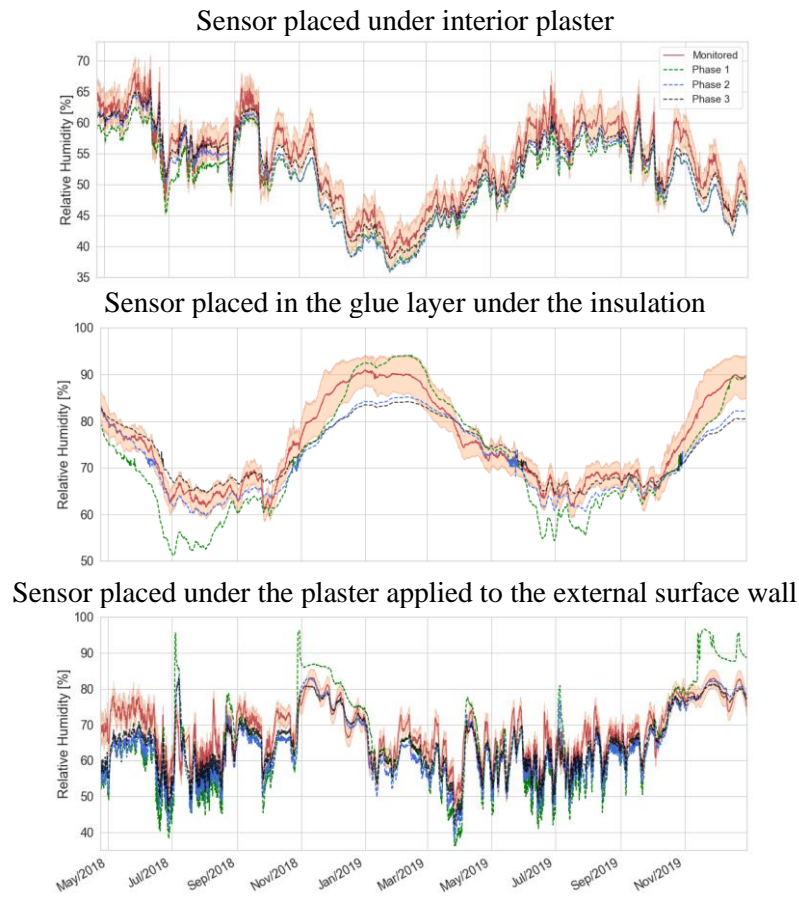
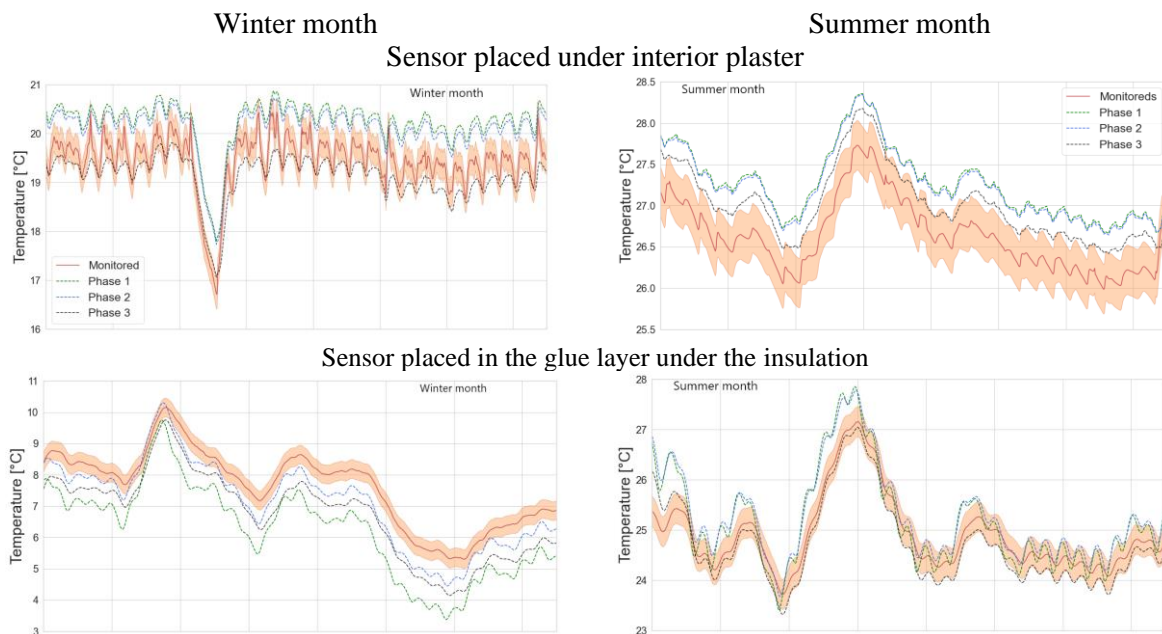


Figure 2. Curves of the relative humidity measured by the sensors in the 3 layers of masonry compared with the one obtained from optimization phases.

The same graphs are also shown for the monitored and simulated temperatures in Figure 3. To obtain a better visualization of the different temperature curves, a specific month is represented in winter (left column) and in summer (right column).



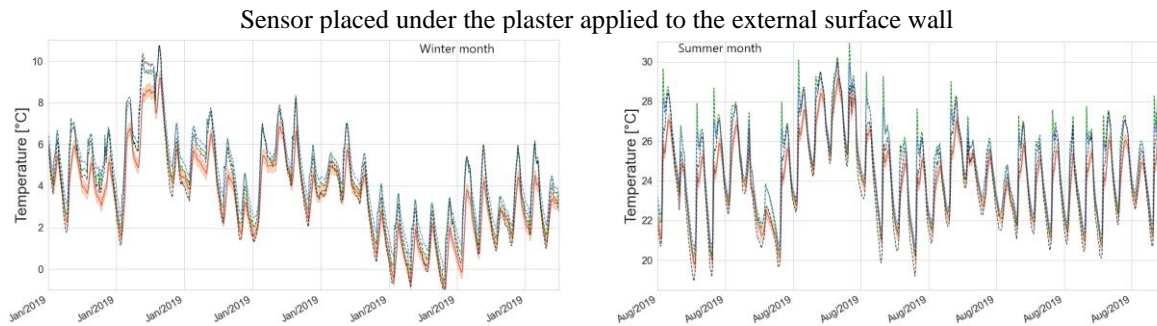


Figure 3. Curves of the temperature [°C] measured by the sensors in the 3 layers of masonry compared with the one obtained from optimization phases. Winter month on the left and summer month on the right

4. Discussion

The overall agreement between the monitored and the simulated curves is quite good already after *Phase 1*, where the input is selected according to the information collected in the materials' datasheets and based on standard values for the coupling coefficients. The trend of the two curves is similar and the main phenomena seems to be captured by the simulation.

Phase 2 improves the situation, leading to a reduction of 17.3% of the thermal RMSE and of 25.5% of the hygrometric RMSE. All the materials obtained after this calibration phase are reasonable if compared with the descriptions contained in the datasheets. The obtained glue is a clay adhesive mortar, which is the same already selected in *Phase 1*. For the old plaster, the lowest RMSE is obtained with a lime-based surface plaster. The most suitable stone was "Sandstone Rütten" which is a sandstone located in the Sauerland area in Germany. The new plaster obtained from the analysis is a plaster based on hydraulic lime, exactly as the actual plaster applied on-site. The procedure of selecting the materials based on the minimization of the RMSE value was performed several times, changing the order in which the materials are optimized and also changing the starting materials. The result was always the same and we always obtained the materials reported in Table 2.

The calibration process performed in *Phase 3* further reduces the thermal and hygrometric RMSE. In this phase, two types of inputs are changed: the material hygrothermal properties and the coupling coefficients with the boundary conditions. The variation of the material hygrothermal properties led to a minor reduction of the RMSE values (-0.65% thermal RMSE and -1.64% hygrometric RMSE) and the step of adapting the material parameters to those present in the respective datasheets even increased the RMSE values (+11.7%, thermal RMSE and +0.6% hygrometric RMSE). Conversely the variation of the coupling coefficient leads to a significant reduction of the RMSE values (17.2% thermal RMSE and 26.1% hygrometric RMSE). It should be noted that the parametric variation of the stone's parameter lead to values that differ significantly from those measured in the laboratory. However, this is considered plausible as the calibration procedure does not consider only the stone itself but also its combination with the historical mortar composing the wall [12].

The overall parameterization process clearly reduces the objective function. An overall reduction of 31.8% is observed for the thermal RMSE and a reduction of 45.9% for the hygrometric RMSE. The graphs show that the simulated curve is moving closer to the monitored curve during the optimization process. Nevertheless, an optimal result is not always observed. For example, the peak value of the relative humidity behind the insulation in winter is reduced far below that monitored in winter (Figure 2). This value is highly important for detecting the possible formation of interstitial condensation. The simulated relative humidity in the layer under the internal and external plaster approaches the humidity recorded by the sensors. In particular, the initial simulation (*Phase 1*) shows anomalous fluctuations in the values (Figure 2) while after the parameterization process (*Phase 2*, *Phase 3*) the simulated curves clearly follows the trend of the monitored one. The temperature curves are in good agreement, but with a slight offset, which is significantly reduced after the parametric analysis of the internal and external heat transfer coefficients, and of the solar radiation absorption coefficient (9%, 5% and 7% respectively).

5. Conclusion

Using a parametric approach, the initial hygrothermal model is calibrated to optimize the agreement with the monitored curves. The overall calibration process led to a significant improvement of the agreement between monitored and simulated curves with a reduction of 31.8% of the thermal RMSE and of 45.9% of the hygrometric RMSE. The overall agreement between the monitored and simulated curves indicates the potential of dynamical hygrothermal simulation in describing the combined transport of moisture and heat in constructions.

At the same time, the all process highlighted some limitations of the used methodology and provided important information for possible improvements. Currently, the method has involved varying a single parameter at a time while holding the others constant. This approach has not proved to be the best. In some cases, the obtained value for one parameter varied to compensate the errors in other parameters. This is supposed to happen when the optimized parameter is obtained as one of the edges of the selected variation range. On the other hand, we believe that the parametric analysis of the materials in the database (*Phase 2*) is an important starting point that has directed the authors towards a model that is close to reality.

This work can be an excellent starting point and basis for a more complex approach involving the variation of several parameters in parallel according to a numerical model that attempts to reduce the chosen statistical index. For this purpose, additional optimization software could be used that performs the parametric analysis having as objective the reduction of the RMSE index.

6. References

- [1] Sandrolini F and Franzoni E 2006 An operative protocol for reliable measurements of moisture in porous materials of ancient buildings *Build. Environ.* **41** 1372–80
- [2] Bastien D and Winther-Gaasvig M 2018 Influence of driving rain and vapour diffusion on the hygrothermal performance of a hygroscopic and permeable building envelope *Energy* **164** 288–97
- [3] Straube K U J and Van Straaten Pe R 2013 Field Monitoring and Simulation of a Historic Mass Masonry Building Retrofitted with Interior Insulation
- [4] Freudenberg P, Ruisinger U and Stöcker E 2017 Calibration of Hygrothermal Simulations by the Help of a Generic Optimization Tool *Energy Procedia* **132** 405–10
- [5] Roberti F, Oberegger U F and Gasparella A 2015 Calibrating historic building energy models to hourly indoor air and surface temperatures: Methodology and case study *Energy Build.* **108** 236–43
- [6] Grint N, Marincioni V and Elwell C A 2020 Sensitivity and Uncertainty analyses on a DELPHIN model: The impact of material properties on moisture in a solid brick wall *E3S Web Conf.* **172** 1–8
- [7] Coelho G B A, Silva H E and Henriques F M A 2018 Calibrated hygrothermal simulation models for historical buildings *Build. Environ.* **142** 439–50
- [8] Delphin 6.1 Technische Universität Dresden . Institut für Bauklimatik .Delphin 6.1 Material Database.
- [9] Anon BS, EN 15026. (2007) Hygrothermal Performance of Building Components and Elements – Assessment of Moisture Transfer by Numerical Simulation. London: British Standards
- [10] WTA 2014 Simulation of heat and moisture transfer
- [11] Danish Standards 2009 Bygningers hygrotermiske ydeevne – Beregning og præsentation af klimadata – Del 3 : Beregning af slagregnsindeks for lodrette overflader ud fra timeværdier for vind og regn
- [12] Bottino-Leone D, Larcher M, Troi A and Grunewald J 2021 Hygrothermal characterization of a fictitious homogenized porous material to describe multiphase heat and moisture transport in massive historic walls *Constr. Build. Mater.* **266** 121497

Acknowledgments

The authors would like to acknowledge the financial support for this research received through the HyLAB project, Project funded by Provincia Autonoma di Bolzano – Alto Adige.